

# Morphology-Related Packetlike Space-Charge Behavior in Linear Low-Density Polyethylene Doped with Al<sub>2</sub>O<sub>3</sub> Nanoparticles

Feihu Zheng, Shujuan Hao, Wenyan Wang, Chun Xiao, Zhenlian An, Yewen Zhang

*Pohl Institute of Solid State Physics, Tongji University, 1239 Siping Road, Shanghai 200092, China*

Received 13 July 2008; accepted 7 October 2008

DOI 10.1002/app.29571

Published online 25 February 2009 in Wiley InterScience (www.interscience.wiley.com).

**ABSTRACT:** Packetlike space-charge behavior and the isothermal decay processes of the injected charge in neat linear low-density polyethylene (LLDPE) and LLDPE doped with Al<sub>2</sub>O<sub>3</sub> nanoparticles were investigated by the pressure wave propagation method. The 1-mm sheet samples, sandwiched by semiconductive electrodes, were submitted to 40 kV/mm of direct current field at various temperatures for 3 h. The charge-injecting rate and the apparent mobility of packetlike space charge under direct-current stress were compared among the samples subjected to different blending processes with or without

nanoparticles. The slight doping concentration showed a significant influence on the space-charge dynamics, with a lower injecting rate and apparent mobility for higher doped samples. The isothermal decay processes of the injected charge indicated trap-modulated features. The phenomena were considered to be related to the changing morphology of the matrix material. © 2009 Wiley Periodicals, Inc. *J Appl Polym Sci* 112: 3103–3109, 2009

**Key words:** charge transport; morphology; nanocomposites; polyethylene (PE)

## INTRODUCTION

Space-charge injection and migration is significant information to insight into the mechanism of their influence on dielectrics aging and breakdown. A number of physics models have been proposed to investigate space-charge dynamics by the development of space-charge mapping techniques, such as pressure wave propagation (PWP) and pulsed electroacoustics. Packetlike space charge dynamics<sup>1–11</sup> are a specific charge dynamics phenomenon in which a monopolar or bipolar charge is injected from electrodes and shifts as a whole packet to counter electrodes under an applied field; they were first identified by Hozumi and coworkers<sup>1,2</sup> in the 1990s. However, to date, the physics mechanism of the generation and migration of packetlike space charge has still puzzled researchers. There exist two typical models to explain the phenomenon. One is based on the different conductivities in front of and

behind the charge packet.<sup>10</sup> The other considers the carrier shifting velocity as a function of the electric field. The packetlike space charge occurs when a negative slope for the carrier shifting velocity against the electric field is met.<sup>5,7</sup> Both the models consider that the mobility and charge amount of the charge packet is material dependent. The interfaces between the electrodes and sample material determine the charge-injecting rate; the distribution of charge trap level and trap density determine the migrating velocity of the injected charge. The structural charge traps partly depend on the material morphology. The significant influence of the polymer morphology on the carrier transportation has been revealed by many authors.<sup>12–15</sup> However, the relationship between the migration of the packetlike space charge and the material morphology has not been revealed. To investigate how the material morphology influences the packetlike space-charge behavior, we examined the charge injection and migration in linear low-density polyethylene (LLDPE) subjected to various blending processes without and with various concentrations of Al<sub>2</sub>O<sub>3</sub> nanoparticles in this study.

## EXPERIMENTAL

The LLDPE used in this study was Exxon-Mobile Chemical (Irving, Texas) 1004, (melt index = 2.8 g/10 min, density = 0.918 g/cm<sup>3</sup>). The Al<sub>2</sub>O<sub>3</sub> inorganic nanoparticles, with an average diameter of 75 nm,

Correspondence to: Y. Zhang (yewenzhang@online.sh.cn).

Contract grant sponsor: National Natural Science Foundation of China; contract grant numbers: 50537040, 50807040.

Contract grant sponsor: Shanghai Committee of Science and Technology; contract grant number: 07DZ22302.

Contract grant sponsor: Program for Young Excellent Talents in Tongji University.

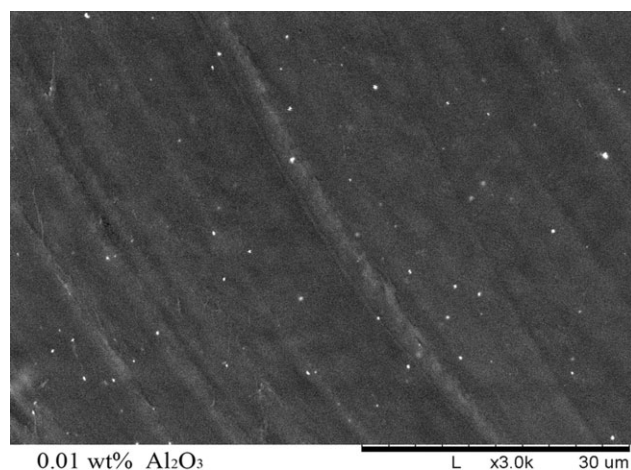


**Figure 1** Scanning electron microscopy image of LLDPE doped with 0.01 wt %  $\text{Al}_2\text{O}_3$ .

were obtained from Degussa (Shanghai, China). The particles were not subjected to any kind of treatment before use. The  $\text{Al}_2\text{O}_3$  nanoparticles were blended with LLDPE particles with a Harpro (Harbin, China) rheometer to prepare six different weight concentrations (0.01, 0.05, 0.1, 0.2, 0.5, and 1 wt %) of  $\text{Al}_2\text{O}_3$ /LLDPE material. The blending process took about 5–6 min at about  $150^\circ\text{C}$ . The profiles of the doped LLDPE were observed by scanning electron microscopy (Fig. 1). It was clear that the inorganic particles were uniformly dispersed in the LLDPE matrix. To evaluate the effect of the blending process at  $150^\circ\text{C}$  on the space-charge behavior, samples of neat LLDPE subjected to a one-time blending process without any nanofiller were also prepared. Both the blended materials and neat LLDPE particles were made into sheet samples by hot-pressing processes at  $130^\circ\text{C}$ . The sheet samples were sandwiched by the semiconductive electrodes made of Ethylene vinyl acetate copolymer (EVA) mixed with carbon black at  $90^\circ\text{C}$  with slight pressure. The averaged thicknesses of sheet samples and the electrodes were 1 and 0.4 mm, respectively.

The samples were submitted to negative  $-40$  kV/mm of direct current field for approximate 3 h at  $40^\circ\text{C}$  and then were short-circuited at the same temperature. The electric field protocol is shown in Figure 2. The space-charge evolution during both processes was monitored by the PWP method. This method uses the pressure pulse as a virtual probe to detect the space-charge distribution in solid dielectrics. In this study, the pressure pulse was generated during the ablation of the surface of the semiconductive electrode, which acted as the infrared pulse laser (Continuum Surelite II-10) [Santa Clara, California] target. The pressure pulse could propagate through the electrode and then across the sample. Under the mechanical disturbance of the pressure

pulse, the displacement of the space charge attached to the atomic structure of the sample produced a current signal in the external circuit. The amplitude of the current signal was proportional to the space-charge density, with a higher current for a higher space-charge density. The full curve of the current against pressure pulse propagation time was obtained when the pressure pulse was propagating through the sample. According to the known velocity of pressure pulses propagating in a sample, the relationship between the pressure pulse propagation instant and its corresponding disturbed position of the sample could be calculated. With Figure 3(a) as an example, peak a and peak b correspond to the interfaces between the electrode and the sample. The curves between peak a and peak b indicate the space-charge distribution in the sample bulk. More details about the PWP method have been described elsewhere.<sup>16</sup>

## RESULTS

### Effect of the blending process

The doped samples prepared by a blending process at  $150^\circ\text{C}$  were subjected to one more heating history than the neat LLDPE sample. Some researchers have reported that the heating history of an insulating polymer may have some influence on the space-charge behavior.<sup>17,18</sup> To determine the influence of the blending process, two neat LLDPE sheet samples were prepared. One of them was subjected to one more blending process without any additive at  $150^\circ\text{C}$  for 10 min. The space-charge behavior in the two samples was compared in this study. The space-charge evolution in the blended and nonblended LLDPE under negative  $-40$  kV/mm of direct current field at  $40^\circ\text{C}$  is presented in Figure 3(a,b). In both cases, the homocharge packets were injected

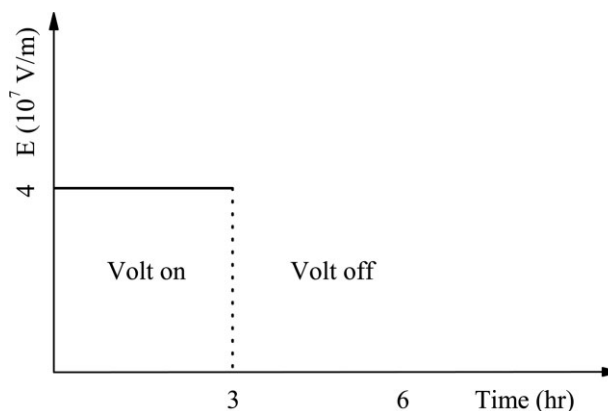


**Figure 2** Electrical field protocol. E invertical axis means applied field.

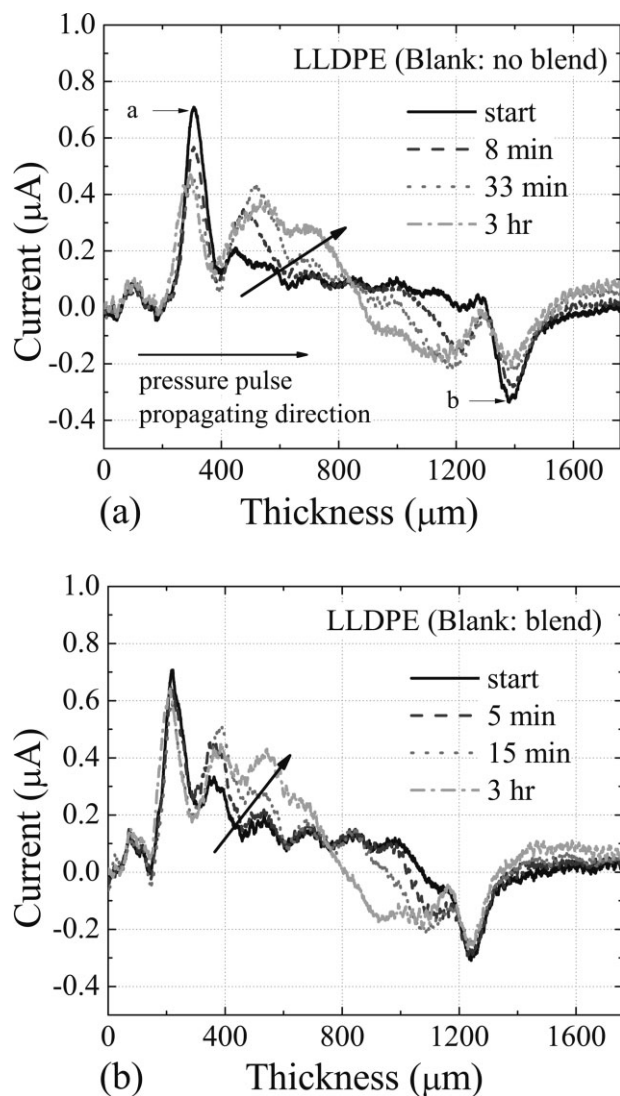


**Figure 3** Space-charge evolution during 3 h of stressing in neat LLDPE samples with and without blending under negative  $-40$  kV/mm of direct current field at  $40^{\circ}\text{C}$ .

from both electrodes and shifted to the counter electrodes, and the total accumulating charge at the same moment was similar. However, the apparent migration velocity of the charge packet in the non-blended sample was slightly higher than that in the blended sample. It seemed that the blending process resulted in a decrease in the apparent mobility of the charge packet.

#### Effect of the nanoparticles

Figure 4 shows the space-charge evolution in the  $\text{Al}_2\text{O}_3/\text{LLDPE}$  samples. The bipolar injecting space-charge packet behavior was observed again in the samples doped with 0.05 and 0.01 wt % nanoparticles. However, the injecting rate in both samples decreased compared with that in the neat sample

(Fig. 3). In addition, the mobility in the 0.05 wt %  $\text{Al}_2\text{O}_3/\text{LLDPE}$  sample was lower than that in 0.01 wt %  $\text{Al}_2\text{O}_3/\text{LLDPE}$  and in the neat sample. The apparent mobility of the charge packet was about on the order of  $10^{-16} \text{ m}^2 \text{ v}^{-1} \cdot \text{s}^{-1}$ . When the doping concentration of nanoparticles increased up to 0.1, 0.2, 0.5, and 1 wt %, the entrance and exit image charge peaks decreased within 3 h of stressing, as shown in Figure 4(c–f). This indicated that the homocharge was slightly injected and accumulated near the electrodes. No visible bulk charge could be found at the amplitude resolution of PWP. The charge-injecting rate was extremely similar among these four samples. However, because of the low charge-injecting rate, the space-charge packet behavior could not be envisaged again. Similar results have been obtained in other oxide nanoparticle/LLDPE samples (not shown in this article). On the basis of the previous analysis, it is clear that the nanoparticle concentration had a significant effect on the space-charge-injecting rate and the charge packet migration in the doped samples.

#### Space-charge decaying process

The charge decay processes at  $40^{\circ}\text{C}$  after the removal of high voltage were studied. Immediately after the high voltage was removed, four typical results with similar homocharges accumulating near the electrodes were observed, as shown in Figure 5, whereas their isothermal decay processes were distinctly different. For the sake of convenience, the space-charge-accumulating region in Figure 5(a–d) is divided into four parts: p1 and p2 correspond to the positive-charge-accumulating regions and n1 and n2 correspond to the negative-charge-accumulating region. As shown in Figure 5(a), the charge in regions p2 and n1 decayed more slowly than the charge in regions p1 and n2 for the neat sample without a blending process. On the contrary, a faster decay process was found in regions p1 and n2, which is shown in Figure 5(b,d). In addition, the decaying rate in the four regions in the LLDPE sample doped with 0.01 wt %  $\text{Al}_2\text{O}_3$  was almost the same [Fig. 5(c)]. The different decay processes were attributed to the different charge mobilities in the samples.

#### DISCUSSION

Many factors, such as applied field, temperature, interface conditions, additives, and material morphology, have impacts on the space-charge behavior. For a given applied field and temperature, the charge-injecting rate is interface dependent, which is determined by the difference in work function between the electrode and sample. The carriers can

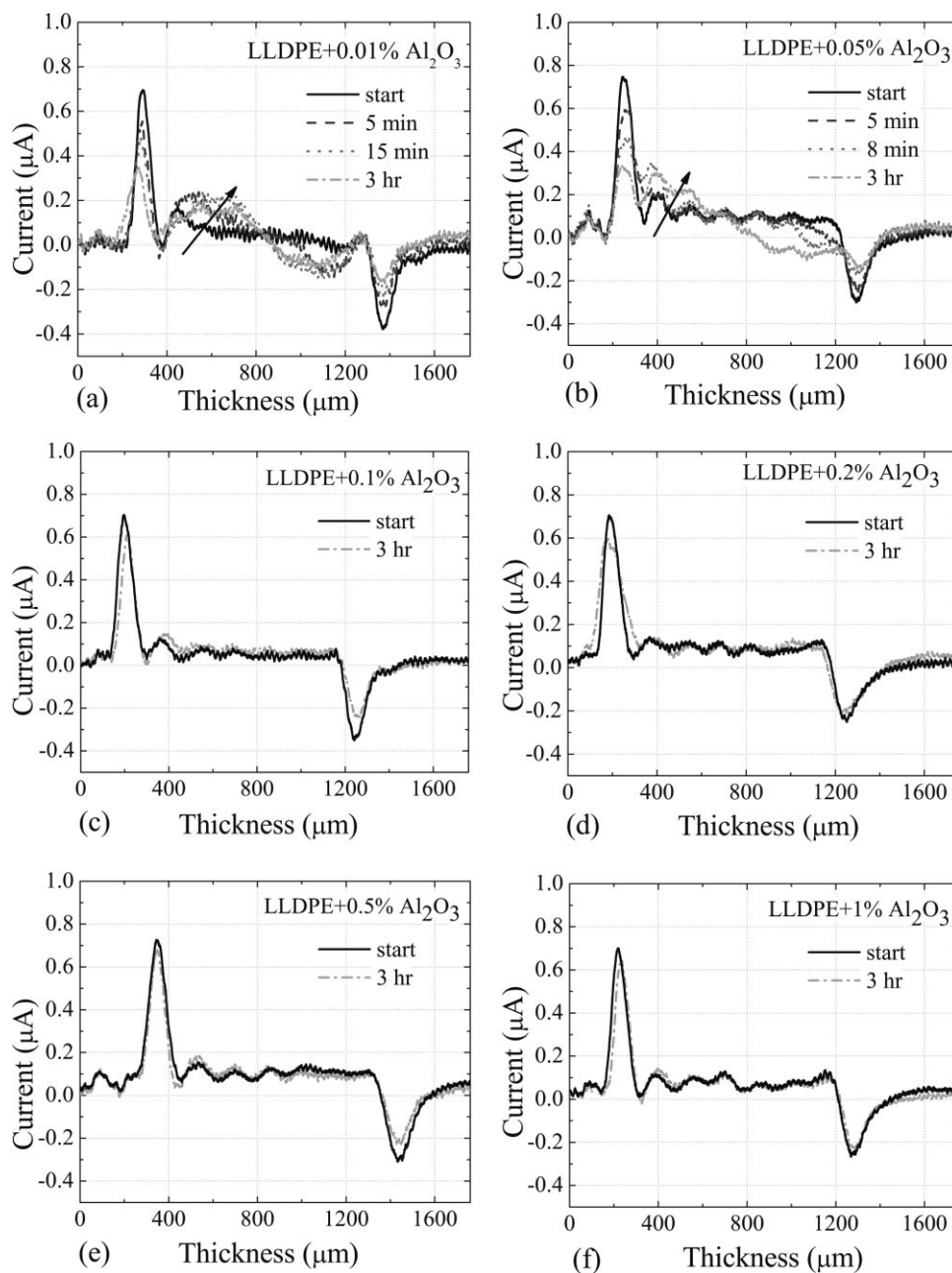


**Figure 4** Space-charge characteristics in LLDPE doped with different concentrations of  $\text{Al}_2\text{O}_3$  nanoparticles: (a) 0.01, (b) 0.05, (c) 0.1, (d) 0.2, (e) 0.5, and (f) 1 wt %. All the samples were subjected to negative  $-40$  kV/mm of direct current field at  $40^\circ\text{C}$  for 3 h.

easily go through the interface when the work function of the two contacted materials is the same. The great charge injection in Figure 3 is thought to have resulted from the approximate work function of the neat sample and the semiconductive electrode. However, for neat samples with different heating histories, Figure 3(a,b) shows different space-charge packet mobilities; this will be discussed in the following section. For the doped samples, the oxide nanofiller in the doped sample enlarged the differences of work function on the interface, and this effect became clearer in the doped sample with higher

concentrations of nanoparticles. Therefore, a lower injecting rate was found in higher doped sample [Figs. 4(c–f)]. On the other hand, the injected space charge was captured by the charge traps. If the injected charge accumulated near the electrodes, the electric field generated by the accumulating charge should have reduced the field on the interface. This would have inversely decreased the successive charge-injecting rate.

The charge accumulation and migration was strongly related to charge trap. Polyethylene is a semicrystalline polymer composed of amorphous

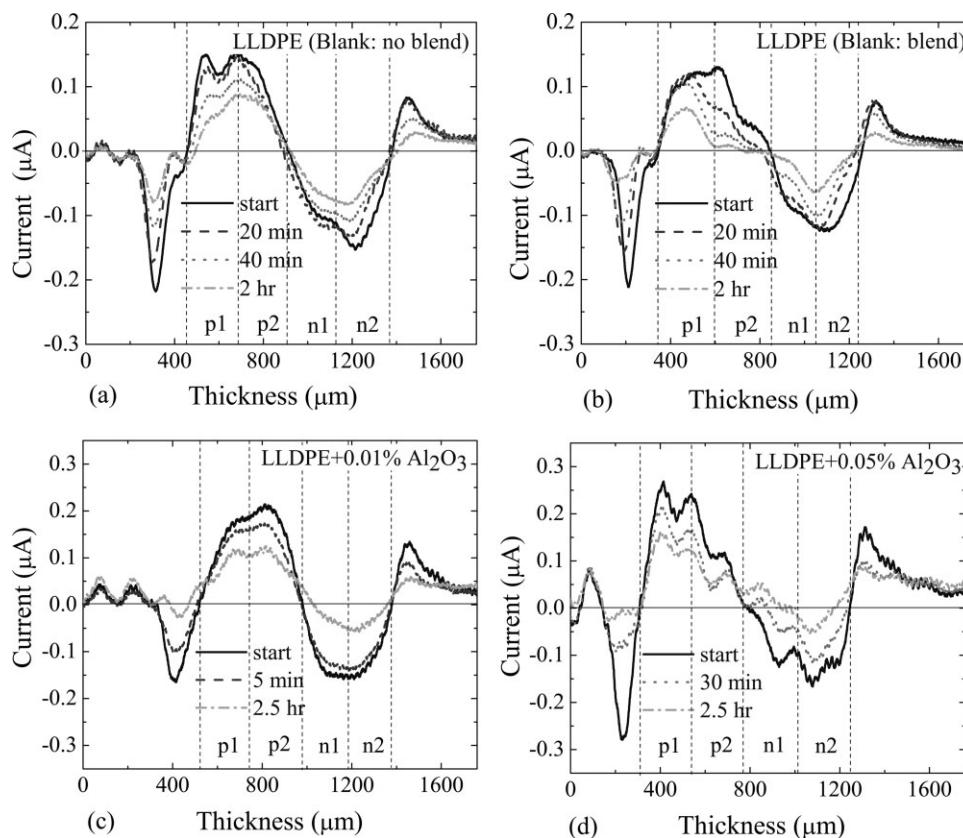


**Figure 5** After the removal of the same high voltage, the space-charge decay processes at 40°C in the samples subjected to different treating processes: neat LLDPE (a) without and (b) with the blending treatment and the LLDPE doped with (c) 0.01 and (d) 0.05 wt %  $\text{Al}_2\text{O}_3$  nanoparticles.

and crystalline regions, and the interfaces of different morphologies can act as structural charge traps.<sup>19</sup> The well-dispersed nanoparticles do not have any nucleating effects,<sup>20</sup> which means that more interfaces between the nanoparticles and amorphous matrix can be generated. For the doped LLDPE, the interfaces between the nanoparticles and LLDPE became new trap centers. Consequently, the charge trap center density became higher in the doped sample than in the neat sample. In addition, our previous work showed that the peak temperature of thermally stimulated discharge shifted to a higher value in the doped sample than in the neat sample,<sup>21</sup> which indicated that the injected charge was captured in the deeper traps. The new deep traps were considered to be located at the amorphous-crystalline interfaces.<sup>19</sup> The carrier mobility ( $\mu$ ) was trap-modulated, which was charge trap level and trap density dependent. It can be expressed with the following equation:<sup>22</sup>

$$\mu = \mu_0 \frac{N}{M} \exp(-U/kT) \quad (1)$$

where  $\mu_0$  is the free carriers mobility, which is a constant less sensitive to temperature, and  $N$ ,  $M$ ,  $U$ , and

$k$  are the vacancy number in the conduction band, the total number of trap centers, the trap level, and the Boltzmann constant, respectively. According to this equation, it was not surprising to find a relative low carrier mobility in the doped LLDPE with higher trap level and trap density. This should have been the reason that we could not observe the going across packetlike space-charge behavior in these samples. A similar phenomenon was found in low-density polyethylene samples doped with MgO nanoparticles.<sup>8</sup> The low mobility also resulted in the injected charge accumulating near the electrodes. Because the charge-injecting rate was related to electric field, the decreasing field due to the homocharge accumulation weakened the charge-injecting rate. Typical results are shown in Figure 4(c–f). The previous equation can also be used to explain the different motilities shown in Figure 3(a,b). The blending process probably changed the material morphology, such as molecular structure and crystallinity; new charge trap centers, therefore, were generated.

The temperature was another parameter that influenced the space-charge migration, as shown in eq. (1). Compared with the space-charge behavior at 40°C, shown in Figure 3(a), a smaller charge

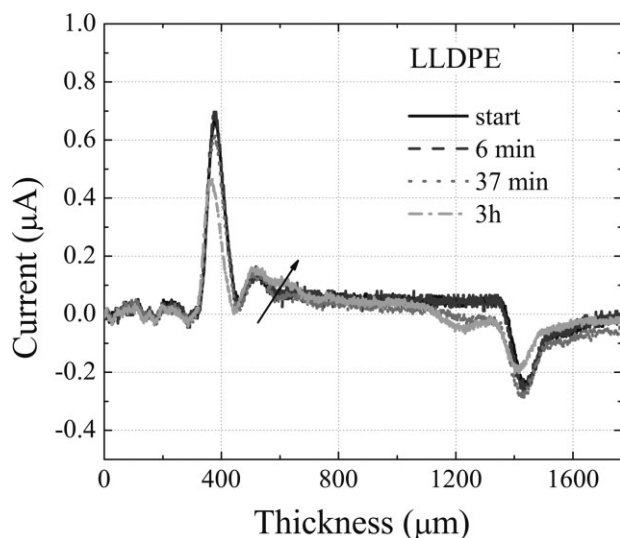


**Figure 6** Space-charge evolution under negative  $-40$  kV/mm of direct current field in the neat LLDPE sample at  $22^{\circ}\text{C}$ .

accumulation and slower migration of the injected charge was found in the sample at  $22^{\circ}\text{C}$  (Fig. 6). The different mobilities at different temperatures can be explained by the following. As mentioned previously, charge migration can be considered as charge moving from one trap site to another trap site (trap-modulated mobility). A higher temperature means that the captured charge could obtain more energy from the environment and, therefore, escape more easily from the traps, which means a shorter interval for the two successive escapes of the captured charges. In other words, a higher temperature could enhance the charge mobility. In the lower temperature case, most of the injected charge accumulated in the vicinity of the electrode and was difficult to shift. This could be the explanation of why space-charge packetlike behavior did not occur at relatively low temperature in the neat LLDPE used in this test.

The charge isothermal decay processes were also trap-modulated. After the removal of high voltage, we visualized that the electric field should have been generated by the accumulating charge. Both of the accumulated positive (regions p1 and p2) and negative (regions n1 and n2) charges could be repelled by the field and move across the position of zero-crossed charge density, which led to bipolar charge decay by the recombination process of the migrating heterocharge (Fig. 5). The recombination should have reduced the charge density in the middle part (regions p2 and n1). For the relatively high mobility among the four samples shown in Figure 5, the charge in regions p1 and n2 continuously shifted and supplemented the charge in regions p2 and n1. Consequently, it seemed that the charge in regions

p1 and n2 decayed faster [Fig. 5(a)]. However, for the relatively low mobility, the process of charge supplements from regions p1 and n2 to regions p2 and n1 became difficult. A faster charge decay process was, therefore, found in regions p2 and n1 [Fig. 5(b,d)]. The most effective charge supplement processes occurred in Figure 5(c). On the basis of the previous analysis, we concluded that the charge apparent mobility in the four samples was in the following order:  $\mu_a > \mu_c > \mu_b > \mu_d$ . This was consistent with the apparent mobility obtained during the high-voltage stressing [Figs. 3(a,b) and 4(a,b)].

## CONCLUSIONS

The bipolar packetlike space-charge behavior and the isothermal charge decay process in neat LLDPE and LLDPE doped with nanooxide particles were investigated. The results show that the blending processes both with and without nanoparticles changed the morphology-related charge trap in the samples, which increased the charge trap density and trap level and, therefore, decreased the apparent mobility of the packetlike space charge. A slight doping concentration (e.g., 0.1 wt %  $\text{Al}_2\text{O}_3$ ) in the  $\text{Al}_2\text{O}_3$ /LLDPE samples significantly reduced the charge-injecting rate and decreased the apparent mobility of the space charge.

## References

- Hozumi, N.; Suzuki, H.; Okamoto, T.; Watanabe, K.; Watanabe, A. *IEEE Trans DEI* 1994, 3, 1068.
- Hozumi, N.; Takeda, T.; Suzuki, H.; Okamoto, T. *IEEE Trans DEI* 1998, 5, 82.
- Kaneko, K.; Mizutani, T.; Suzuoki, Y. *IEEE Trans DEI* 1999, 6, 152.
- See, A.; Dissado, L. A.; Fothergill, J. C. *IEEE Trans DEI* 2001, 8, 859.
- Jones, J. P.; Llewellyn, J. P.; Lewis, T. J. *IEEE Trans DEI* 2005, 12, 951.
- Delpino, S.; Fabiani, D.; Montanari, G. C.; Dissado, L. A.; Laurent, C.; Teyssedre, G. In *Proceedings of the Conference on Electrical Insulation and Dielectric Phenomena*, Vancouver, British Columbia, Canada, Institute of Electrical and Electronics Engineers (IEEE), New York, NY, 2007; p 421.
- Dissado, L. A.; Zadeh, S.; Fothergill, J. C.; See, A. In *Proceedings of the Conference on Electrical Insulation and Dielectric Phenomena*, Vancouver, British Columbia, Canada, Institute of Electrical and Electronics Engineers (IEEE), New York, NY, 2007; p 425.
- Maezawa, T.; Taima, J.; Hayase, Y.; Tanaka, Y.; Takada, T.; Sekiguchi, Y.; Murata, Y. In *Proceedings of the Conference on Electrical Insulation and Dielectric Phenomena*, Vancouver, British Columbia, Canada, Institute of Electrical and Electronics Engineers (IEEE), New York, NY, 2007; p 271.
- Fukuma, M.; Fukunaga, K.; Laurent, C. *Appl Phys Lett* 2006, 88, 253110.

10. Matsui, K.; Tanaka, Y.; Takada, T.; Maeno, T. *IEEE Trans DEI* 2008, 15, 841.
11. Zheng, F.; Zhang, Y.; Gong, B.; Zhu, J.; Wu, C. *Sci Chin Ser E* 2005, 48, 354.
12. Amarasinghe, G.; Chen, F.; Genovese, A.; Shanks, R. A. *J Appl Polym Sci* 2003, 90, 681.
13. Tanaka, Y.; Chen, G.; Zhao, Y.; Davies, A. E.; Vaughan, A. S.; Takada, T. *IEEE Trans DEI* 2003, 10, 148.
14. Chong, Y. L.; Chen, G.; Hosier, I. L.; Vaughan, A. S.; Ho, Y. F. *IEEE Trans DEI* 2005, 12, 1209.
15. Tebani, M.; Boudou, L.; Guastavino, J. *J Appl Polym Sci* 2008, 109, 2768.
16. Laurenceau, P.; Dreyfus, G.; Lewiner, J. *Phys Rev Lett* 1977, 38, 46.
17. Wang, X.; Tu, D.; Tanaka, Y.; Muronaka, T.; Takada, T.; Shinoda, C.; Hashizumi, T. *IEEE Trans DEI* 1995, 2, 467.
18. Pawlowski, T.; Lang, S. B.; Fleming, R. J. In *Proceedings of the Conference on Electrical Insulation and Dielectric Phenomena*, Boulder, CO, Institute of Electrical and Electronics Engineers (IEEE), New York, NY, 2004; p 93.
19. Zhang, Y.; Li, J.; Zheng, F.; Peng, Z.; Wu, C.; Xia, Z. *Chin Phys Lett* 2002, 19, 1191.
20. Huang, X.; Jiang, P.; Kim, C.; Duan, J.; Wang, G. *J Appl Polym Sci* 2008, 107, 2494.
21. Gong, B.; Zhang, Y.; Zheng, F.; Xiao, C.; Wu, C. *Chin J Mater Sci Technol* 2006, 24, 109.
22. Spears, W. E. *J Non-Cryst Solids* 1969, 1, 197.